



## Research article

# Cytoprotective potentialities of carvacrol and its nanoemulsion against cisplatin-induced nephrotoxicity in rats: development of nano-encapsulation form



Tamer I.M. Ragab<sup>a</sup>, Khairy M.A. Zoheir<sup>b</sup>, Nadia A. Mohamed<sup>c</sup>, Abd El-Nasser G. El Gendy<sup>d</sup>, Ahmed M. Abd-ElGawad<sup>e</sup>, Mohamed F. Abdelhameed<sup>f,\*</sup>, Abdel Razik H. Farrag<sup>g</sup>, Abdelsamed I. Elshamy<sup>h,\*\*</sup>

<sup>a</sup> Chemistry of Natural and Microbial Products Department, National Research Centre, Dokki, Giza 12622, Egypt

<sup>b</sup> Cell Biology Department, Biotechnology Research Institute, National Research Centre, Dokki, Giza 12622, Egypt

<sup>c</sup> Medical Biochemistry Department, National Research Centre, Cairo, Egypt

<sup>d</sup> Medicinal and Aromatic Plants Research Department, National Research Centre, 33 El Bohouth St., Dokki, Giza 12622, Egypt

<sup>e</sup> Department of Botany, Faculty of Science, Mansoura University, Mansoura 35516, Egypt

<sup>f</sup> Pharmacology Department, National Research Centre, Dokki, Giza 12622, Egypt

<sup>g</sup> Department of Pathology, National Research Centre, 33 El Bohouth St. Dokki, Giza 12622, Egypt

<sup>h</sup> Chemistry of Natural Compounds Department, National Research Centre, 33 El Bohouth St., Dokki, Giza, 12622, Egypt

## ARTICLE INFO

## Keywords:

Cytoprotective  
Cisplatin-induced nephrotoxicity  
Carvacrol  
Carvacrol-nanoemulsion  
Nanoemulsion  
Histopathology  
Western blot

## ABSTRACT

Cisplatin (Cisp) is a widely distributed chemotherapeutic drug for cancers. Nephrotoxicity is one of the most common side effects of the use of this drug. Carvacrol (CV) is a common natural compound in essential oils and extracts of medicinal plants with potent *in vivo* and *in vitro* bioactivities. The work was extended to achieve the target of investigation of the protective potentialities of CV and its nanoemulsion as a cytoprotective drug against Cisp-induced nephrotoxicity in albino rats. CV-nanoemulsion was prepared by a hydrophilic surfactant polysorbate 80 (Tween 80) and deionized water. The TEM image of the particle distribution prepared nanoemulsion is mainly spherical in shape with particle size varying between 14 and 30 nm. Additionally, the Cisp administration caused the increasing of the levels of urea and creatinine in the blood and serum. These increasing of urea and creatinine levels caused consequently the turbulence of the oxidative stress as well as the rising of hs-CRP, IL-6, and TNF- $\alpha$  levels in the serum. Also, histopathological changes of the kidney tissue were observed. These changes back to normal by treatment with CV-nanoemulsion. Expression levels of nephrotoxicity-related genes including LGALS3, VEGF, and CAV1 in kidney tissue using qRT-PCR were measured. The results revealed that the expression of LGALS3, VEGF and CAV1 genes was highly significantly increased in only Cisp treated group when compared with other treated groups. While, these genes expressions were significantly decreased in Cisp + CV treated group when compared with Cisp treated rats ( $P < 0.001$ ). In addition, there were no significant differences between Cisp + nano-CV treated group and both negative control and nanoemulsion alone groups but it was not significant. In addition, the Western blot of protein analysis results showed that the LGALS3 and CAV1 are highly expressed only in Cisp + CV treated group compared with other groups. There was no significant difference between Cisp + nano-CV treated animals and negative control for both mRNA and protein expression. Based on these results, CV was combined with calcium alginate; a more stable capsule is formed, allowing for the formation of a double wall in the microcapsule. These results supported the therapeutic effect of CV and its nano-emulsion as cytoprotective agents against Cisp nephrotoxicity.

\* Corresponding author.

\*\* Corresponding author.

E-mail addresses: [fayed.nrc@gmail.com](mailto:fayed.nrc@gmail.com), [mf.abdelhameed@nrc.sci.eg](mailto:mf.abdelhameed@nrc.sci.eg) (M.F. Abdelhameed), [elshamynrc@yahoo.com](mailto:elshamynrc@yahoo.com) (A.I. Elshamy).

## 1. Introduction

Cancer can be topped the major health risks worldwide, a principal cause of disease related morbidity and mortality worldwide [1]. The reported cancer risks related morbidity are not due to the underlying disease itself but also include the chemotherapy effects. It is noteworthy that oncologists are obliged to prescribe conventional chemotherapeutic drugs as the first-line agents in treating various malignancies but this hope soon comes to disappointment due to the action of harmful chemicals causing kidney toxicity [2].

Drug-induced nephrotoxicity is still unavoidable in the clinical situation due to its association with several factors that include drug overdose, drug-drug interactions and drug-related adverse effects. The successful cooperation between scientists and clinicians in detecting and understanding the specific pathogenic mechanisms of nephrotoxic drugs, as well as medical monitoring and early detection of drug-induced nephrotoxicity are critical in decreasing the incidence of kidney injury and realistic approaches to avoid the end stage of renal failure [3].

The kidney, an essential organ in human body, is main target for drug-induced toxicity with responsibility to eliminate xenobiotics and metabolic products from the blood into the urine [4]. This process was occurred via three important successive functions glomerular filtration, tubular reabsorption and secretion of substances [4]. During these physiological functions, the kidney compartments especially renal proximal tubular cells (PTC) are naturally subjected to high concentrations of metabolites as well as drugs susceptible to drug toxicity [5, 6]. Drug toxicity may be increased up to 60% in elderly patients within the acute kidney injury (AKI), chronic kidney disease (CKD) and acute renal failure (ARF) and thus end-stage renal disease (ESRD) [7, 8, 9]. All these ailments were occurred via common the pathogenic nephrotoxicity mechanisms including included alteration of intra-glomerular hemodynamics, tubular cell toxicity, inflammation, crystal nephropathy, rhabdomyolysis, and thrombotic micro-angiopathy [7].

Cisplatin [cis-diamminedichloroplatinum II, Cisp] is a drug that displays multi-organ toxicity with its potential cytotoxic mechanisms via oxidative stress, inflammation and apoptotic and DNA degeneration action [10]. It is one of the highly effective and most used antineoplastic platinum-containing chemotherapeutic drugs [10]. Nephrotoxicity is reckoned as the main and specific dose-limiting side effect of Cisp. This drug is cleared in the kidney by both tubular secretion and glomerular filtration. The proximal tubules are the main target for Cisp in the kidney, as it accumulates and causes cellular damage [11]. The *in vivo* Cisp-induced nephrotoxicity is multi-mechanistic involve oxidative stress, inflammation, fibro-genesis, and apoptosis. High doses of Cisp result in proximal tubules cell necrosis, while low doses result in apoptosis [12]. The development of less nephrotoxic drugs is defying because the prediction of nephrotoxicity during drug development remains difficult. But the hope lies in combination of herbal medication with targeted drugs [13]. So, the prevention and/or decreasing of the side effects of drugs are of the main concerns in treating patients who are forced to take them for long periods or permanently. The present study elucidates a new way to get these treatments without subjecting them to new drug toxicity.

Carvacrol (CV, 5-isopropyl-2-methylphenol) is a common monoterpenoid and widely distributed in the essential oils (EOs) derived from the members of the plant kingdom [14]. CV represented the main component of the EOs of several plant species such as *Origanum vulgare* (Fam.: Lamiaceae) [15], *Thymus vulgaris* (Fam.: Lamiaceae) [16], *Lepidium flavum* (Fam.: Brassicaceae), *Stellera chamaejasme* (Fam.: Thymelaeaceae) [17], *Citrus aurantium* (Fam.: Rutaceae), and others [14].

Many biological and pharmaceutical potentialities were documented for CV like antimicrobial, including antifungal, antibacterial, and antiviral [18, 19, 20, 21, 22], anticancer [23, 24, 25], free radical scavenging activity [26, 27, 28], hepatoprotective [29], antinociceptive [27], antiplatelet [30], and antimutagenic [31]. CV is a potent inhibitor of food-borne pathogens as *Bacillus cereus*, *Salmonella*, and *Escherichia coli* [14]. In clinical trial studies, CV was reported to have a significant potentiality in reducing the irritant sensation thus producing self-desensitization *via* repeated use [32].

Herein, this work aims to the evaluation of the nephron-protection potentialities of CV and its nanoemulsion against Cisp-induced toxicity in male albino rats based upon i) biochemical, ii) histopathological, iii) gene expression and iv) Western blot analysis.

## 2. Materials and methods

### 2.1. Chemicals and drugs

Carvacrol (CV) and Cisplatin were purchased from Sigma Aldrich (Merck, Darmstadt, Germany) and WC Heraeus GmbH & Co., KG (Hanau, Germany), respectively. All the used chemicals in this present work were in the highest grade.

Blood urea and serum creatinine (kinetic method), all mentioned kits were supplied from Spectrum chemical company (New Brunswick, USA). While tumor necrosis factor alpha (TNF- $\alpha$ ), interleukin 6 (IL-6), and hypersensitive C-reactive protein (hs-CRP) ELISA Kits were purchased from Bioneovan Company (Beijing, China).

### 2.2. CV-nanoemulsion preparation

A nanoemulsion of the CV was prepared using Tween 80 as a non-ionic surfactant derived from sorbitan esters. Tween 80 was added to EO (1:1 w/w) as the organic phase. The mixture of the organic phase was slowly added in droplets to distilled water (aqueous phase) with vigorously stirring via stirring device at 25 °C overnight. The prepared emulsion was sonicated at 20 °C for 15 min using Ultrasonic (Sonics & Materials, Inc., 53 Church Hill Rd., Newtown, CT, USA) with a probe diameter of 13 mm at a high frequency of 20 kHz and power output of 750 W [33].

### 2.3. Transmission electron microscopy (TEM)

Particle size and shape of the CV-nanoemulsion were determined with a JEOL JEM 1011 (Japan) transmission electron microscope. A 400  $\mu$ L of nanoparticle solutions were deposited on carbon coated copper grids (400 meshes) and dried at 30 °C before image capture [34].

### 2.4. Animals and ethical statements

In the present study, we used ~150 g male albino rats that feed with standard laboratory food and water ad libitum. The protocol was performed in accordance with the Ethics Committee at the National Research Centre, Egypt, taking into consideration the recommendations of the US National Institutes of Health Guide for Care and Use of Laboratory Animals (Publication No. 85-23, revised; approval no: 17-129).

### 2.5. Experimental design

Rats were randomly categorized into six equal groups, with six rats each. The rats' treatment and the experimental design were performed according to Table 1. The Cisp induction was performed according to Shalaby et al., 2021 one month [35]. At the end of the experiment, rats were euthanized by decapitation, and blood and kidney tissues were collected. A portion of the tissues were fixed in neutral buffered formalin (10%) for histopathological examination, while the rest were quickly dissected on the ice-cold plate, washed with ice-cold normal saline, and stored at -80 °C for the biochemical analyses. The kidney was regulated with 0.1 M saline phosphate buffer (pH 7.4) to give a final concentration of 20% (w/v) to examine the biochemical assays.

### 2.6. Biochemical analyses

#### 2.6.1. Assay of lipid peroxidation, reduced glutathione (GSH), and superoxide dismutase (SOD)

Lipid peroxidation in the kidney tissue was determined by measuring the content of the malondialdehyde (MDA) [36]. In this assay, the

**Table 1.** Animal experimental design.

Experimental design	
Group	Treatment
Group I (Control group)	the rats were intraperitoneal injected (I.P.) with saline only.
Group II (Cisp. group)	the rats were provided with 20 mg kg <sup>-1</sup> Cisp [35]
Group III (CV only)	the rats have injected with 150 mg kg <sup>-1</sup> CV,
Group IV (CV-nanoemulsion only)	the rats were injected with 150 mg kg <sup>-1</sup> CV-nanoemulsion.
Group V (CV/Cisp.)	the rats were injected with 150 mg kg <sup>-1</sup> CV + Cisp.
Group VI (CV-nanoemulsion/Cisp.)	the rats were injected with 150 mg kg <sup>-1</sup> CV-nanoemulsion + Cisp.

The rats were injected three times/week for one month while in groups V and VI the rats were administered for three weeks alone before the injection of cisp. and then were continued for one week.

thiobarbituric acid reactive substances react with thiobarbituric acid, producing a red-colored complex that can be assayed via determination of its absorbance at 532 nm by a spectrophotometer. On the other hand, GSH content was determined in brain tissue using the method of El-Refaei et al. [37]. In this assay, the Ellman's reagent is reduced by the -SH groups of GSH to produce a yellow-colored 2-nitro-5-mercaptobenzoic acid, where the intensity of the color can be measured at 412 nm via the spectrophotometer. The SOD activity was estimated according to Mohamed and Fayed [38]. Units of SOD activity were expressed as the amount of enzyme needed to inhibit the reduction of nitroblue tetrazolium (NBT) by 50%, and the activity was expressed as units per mg protein.

### 2.6.2. Assays for kidney functions

The blood urea and serum creatinine were determined via kits (Spectrum chemical company, New Brunswick, USA) according to the kinetic method as mentioned by Salama et al. [39].

### 2.6.3. Assays for inflammatory indexes of the treated rats

The tumor necrosis factor alpha (TNF- $\alpha$ ) was assayed according to the methods of Abd El-Karim et al. [40], interleukin 6 (IL-6) was assayed according to Ghanim et al. [41], and hypersensitive C-reactive protein (hs-CRP) levels were measured according to Sakyi et al. [42]. These assays were performed by ELISA Kits were purchased from Bioneovan Company (Beijing, China).

### 2.7. Histopathological examination

At the end of the experiment, kidney and liver tissues were removed and fixed in formalin (10%). After 24 h, the tissues were gradually dehydrated via ethanol (70% to absolute), then cleared in xylene, impregnated, and embedded in paraffin wax. Sections were prepared using a microtome, stained with hematoxylin and eosin (H&E), and mounted by DPX. The prepared slides were examined for microscopic alterations by light microscopy [43].

### 2.8. Gene expression analysis

#### 2.8.1. RNA extraction and cDNA synthesis

All the extraction procedures were achieved on ice using ice-cold reagents. The total RNA from kidney tissue was isolated using TRIzol reagent (Invitrogen) according to the manufacturer's instructions and quantified by measuring the absorbance at 260 nm. The RNA quality was determined by measuring the 260:280 ratios. The isolated RNA was converted into cDNA using cDNA synthesis kit (Thermo Scientific). Complementary DNA (cDNA) synthesis was performed using a High-Capacity cDNA Reverse Transcription kit (Applied Biosystems) according to the manufacturer's instructions. Briefly, 1.0  $\mu$ g of total RNA from

each sample was added to a mixture of 2.0  $\mu$ l of 10 $\times$  reverse transcriptase buffer, 0.8  $\mu$ l of 25 $\times$  dNTP mix (100 mM), 2.0  $\mu$ l of 10 $\times$  reverse transcriptase random primers, 1.0  $\mu$ l of MultiScribe reverse transcriptase and 3.2  $\mu$ l of nuclease-free water. The final reaction mixture was kept at 25  $^{\circ}$ C for 10 min, heated to 37  $^{\circ}$ C for 120 min, heated at 85  $^{\circ}$ C for 5 s, and finally cooled to 4  $^{\circ}$ C.

#### 2.8.2. Quantitative real-time PCR

The forward primer sequence for Lgals3 expression analysis was 5'-GGAGCACTAACCCAGGAAAATGG-3', and the reverse primer was 5'-GAAGCGGGGGTTAAAGTGG-3'. The forward primer for VEGFA expression analysis was 5'-TCCAATTGAGACCTGGTGA-3', and the reverse primer was 5'-AAGGCTCACAGTGAACGCTCC-3'. The forward primer for Cav1 expression analysis was 5'-TGAACCTCTTCTCCACCGC-3', and the reverse primer was 5'-AGATGCCGTCGAACTGTGT-3'. Real-time PCR was performed in QuantStudio<sup>TM</sup> 7 Flex Real-Time PCR System (Thermo Scientific), using PowerUp<sup>TM</sup> SYBR<sup>®</sup> Green Master Mix (Thermo Scientific). GAPDH was used as an internal control. The 2<sup>- $\Delta\Delta$ CT</sup> method was used to calculate the relative expression of the gene.

User Bulletin No. 2. Briefly, the data are presented as the fold change in gene expression normalized to the endogenous reference gene ( $\beta$ -actin) and relative to a calibrator. Each experiment was conducted in triplicate and repeated three times independently.

### 2.9. Western blot analysis

The Ready Prep<sup>TM</sup> protein extraction kit (total protein) provided by Bio-Rad Inc (Catalog #163-2086) was employed according to manufacturer instructions was added to each homogenized sample of all different groups. Bradford Protein Assay Kit (SK3041) for quantitative protein analysis was provided by Bio basic inc (Markham Ontario L3R 8T4 Canada). A Bradford assay was performed according to manufacture instructions to determine protein concentration in each sample. 20  $\mu$ g protein concentration of each sample was then loaded with an equal volume of 2x Laemmli sample buffer containing 4% SDS, 10% 2-mercaptoethanol, 20% glycerol, 0.004% bromophenol blue, and 0.125 M Tris HCl. The pH was checked and brought to 6.8. Each previous mixture was boiled at 95  $^{\circ}$ C for 5 min to ensure denaturation of protein before loading on polyacrylamide gel electrophoresis. Polyacrylamide gels were performed using TGX Stain-Free<sup>TM</sup> FastCast<sup>TM</sup> Acrylamide Kit (SDS-PAGE), which was provided by Bio-Rad Laboratories Inc Cat # 161-0181. The SDS-PAGE TGX Stain-Free FastCast was prepared according to manufacture instructions. The gel was assembled in a transfer sandwich as follows from below to above (filter paper, PVDF membrane, gel, and filter paper). The sandwich was placed in the transfer tank with 1x transfer buffer, which is composed of 25 mM Tris and 190 mM glycine, and 20% methanol. Then, the blot was run for 7 min at 25 V to allow protein bands to transfer from gel to membrane using BioRad Trans-Blot Turbo. The membrane was blocked in tris-buffered saline with Tween 20 (TBST) buffer and 3% bovine serum albumin (BSA) at room temperature for 1 h. The components of the blocking buffer were as follows; 20 mM Tris pH 7.5, 150 mM NaCl, 0.1% Tween 20, and 3% bovine serum albumin (BSA). Primary antibodies of CAV1 and LGALS3 were purchased from Invitrogen (Carlsbad, CA, USA). Primary antibodies were diluted in TBST according to manufactured instructions. Incubation was done overnight in each primary antibody solution, against the blotted target protein, at 4  $^{\circ}$ C. The blot was rinsed 3–5 times for 5 min with TBST. Incubation was done in the HRP-conjugated secondary antibody (Goat anti-rabbit IgG-HRP-1mg Goat mab-Novus Biologicals) solution against the blotted target protein for 1 h at room temperature. The blot was rinsed 3–5 times for 5 min with TBST.

The chemiluminescent substrate (Clarity<sup>TM</sup> Western ECL substrate Bio-Rad cat#170-5060) was applied to the blot according to the manufacturer's recommendation. Briefly, equal volumes were added from solution A (Clarity western luminal/enhancer solution) and solution B (peroxidase solution). The chemiluminescent signals were captured

using a CCD camera-based imager. Image analysis software was used to read the band intensity of the target proteins against the control sample  $\beta$ -actin (housekeeping protein) by protein normalization on the ChemiDoc MP imager. All fold changes of band densities were determined with normalization to  $\beta$ -actin, an endogenous control. Relative protein expression was calculated as the relative density of a protein band normalized to the endogenous control. Each experiment was conducted in triplicate and repeated three times independently.

### 2.10. CV-encapsulation preparation

CV-encapsulation was encapsulated by cross-linking in calcium alginate beads. Sodium alginate (2 mL; 4%) and 0.5 mL of the CV-encapsulation (0.02 gm) were dissolved in 0.1 M acetate buffer and then, the resulted viscous mixture was dropped (with suitable dropper) into cold calcium chloride solution (20 mL; 0.2M). The formed calcium alginate beads (comprising the CV-encapsulation) were stored in a refrigerator for 24 h, and then the unbounded CV-encapsulation was removed by washing with distilled water [44].

### 2.11. Statistical analysis

Data are presented as mean  $\pm$  SE. Differences between groups were evaluated using one-way analysis of variance (ANOVA), followed by Duncan's multiple range test using SPSS software (SAS Institute Inc., Cary, NC). Differences were regarded as statistically significant at a probability value of less than 0.05.

## 3. Results

### 3.1. Transmission electron microscopy (TEM) of CV-nanoemulsion

The shape and size of the prepared CV-nanoemulsion were evaluated using the HRTEM technique. CV-nanoemulsion was prepared by a hydrophilic surfactant polysorbate 80 (Tween 80) and deionized water. Figure 1 displays the TEM image of the particle distribution of the prepared nanoemulsion. The prepared nanoemulsion is mainly spherical in shape with particle size varying between 14 and 30 nm. The particles are separated from each other which reflects the capping action of the nanoemulsion in the preparation process. The mean droplet size diameter of CV-nanoemulsion was 106 nm (25%  $\leq$  62 nm, while 75%  $\leq$  153 nm

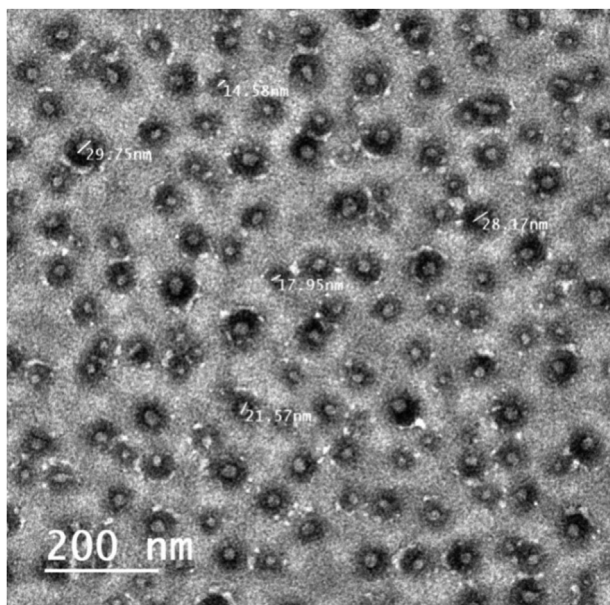


Figure 1. TEM image of CV-nanoemulsion particles distribution.

[33]. Both Tween 80 concentration and time of sonication displayed the main role in the formation of nanoemulsion [45]. The droplets of nanoemulsion have a size ranging from 20 to 200 nm [46]. Felicio et al., 2021 [47] described that the nanoemulsion of carvecrol prepared under the same conditions is stable with the zeta potential ranges of  $-26.37$  to  $-14.60$ . It has been reported that the small droplet size of nanoemulsion can be recognized when the surfactant hydrophile lipophile balance (HLB) value coincides with the value of the essential oil [48].

### 3.2. Effect of CV and its nanoemulsion on oxidative stress, SOD, GSH, and MDA in cisp-induced nephrotoxicity in rats

The mean values of kidney SOD and GSH, in CV and nanoemulsion groups, were insignificantly changed compared to the control group, the recorded mean value of SOD, GSH in the control positive group was significantly decreased compared to the control group (Table 2). While the mean values of kidney SOD and GSH in CV/Cisp and CV-nanoemulsion/Cisp groups were significantly decreased compared to the control group. In contrast, the mean values of (MDA) in cisp group were significantly increased compared to the control group.

### 3.3. Effect of CV and its nanoemulsion on kidney functions in cisp-induced nephrotoxicity in rats

Induction of nephrotoxicity in experimental animals (Cisp group) caused the serum urea, creatinine was significantly elevated in comparing with the control group. Meanwhile, nephrotoxic animals that were protected with CV-nanoemulsion recorded a less observable increase in serum urea, creatinine compared to NC animals indicating a better improvement. On the other hand, no significant difference in the level of serum urea, and creatinine were observed between rats treated with either CV or its nanoemulsion and normal control animals (Table 3).

### 3.4. Effect of CV and its nanoemulsion on serum Hs-CRP, IL-6, and TNF- $\alpha$ in cisp-induced nephrotoxicity in rats

Induction of nephrotoxicity in experimental animals (Cisp group) caused the significant elevation of the serum levels of hs-CRP, IL-6, and TNF- $\alpha$  in comparison to the control group (Table 4). Meanwhile, nephrotoxic animals protected with CV-nanoemulsion recorded a less observable increase in serum hs-CRP, IL-6, and TNF- $\alpha$  compared to normal control rats indicating a better improvement. On the other hand, no significant difference in the level of serum hs-CRP, IL-6 and TNF- $\alpha$  were observed between rats treated with either CV or its nanoemulsion and normal control animals.

### 3.5. Histopathological results of the kidney tissue

Microscopic examination of the tissue from the renal cortex of control rats showed normal renal corpuscles, proximal convoluted tubules, and distal convoluted tubules. The glomeruli, urinary spaces, and Bowman's

Table 2. Effect of CV and its nanoemulsion on MDA, SOD, and GSH in kidney tissue in Cisp-induced nephrotoxicity in rats.

Groups	MDA (nmol/g)	SOD (ug/g)	GSH (ug/g)
Control	0.79 $\pm$ 0.04	191.1 $\pm$ 3.7	31.3 $\pm$ 0.7
Cisp group	1.33 $\pm$ 1.04 <sup>a</sup>	135.4 $\pm$ 2.4 <sup>a</sup>	15.4 $\pm$ 0.3 <sup>a</sup>
CV	0.78 $\pm$ 0.04 <sup>b</sup>	189.3 $\pm$ 4.1 <sup>b</sup>	29.3 $\pm$ 0.6 <sup>b</sup>
CV-nanoemulsion	0.84 $\pm$ 0.04 <sup>b</sup>	188.4 $\pm$ 4.1 <sup>b</sup>	27.4 $\pm$ 0.3 <sup>b</sup>
CV/Cisp	1.07 $\pm$ 0.07 <sup>a</sup>	153.5 $\pm$ 3.4 <sup>a</sup>	22.7 $\pm$ 0.3 <sup>a</sup>
CV-nanoemulsion/Cisp	0.94 $\pm$ 0.07 <sup>a</sup>	179.3 $\pm$ 1.7	25.4 $\pm$ 0.4 <sup>a</sup>

Values are represented as means  $\pm$  SE for 6 rats in each group. <sup>a</sup> significant difference compared to control group, <sup>b</sup> significant difference compared to Cisp.group. Significant at P < 0.05 (one-way ANOVA).

**Table 3.** Effect of CV and its nanoemulsion on kidney functions in Cisp-induced nephrotoxicity in rats.

Groups	Urea mg/dl	Creatinine mg/dl
Control	20.4 ± 0.74	0.58 ± 0.03
Cisp group	45.7 ± 1.07 <sup>a</sup>	2.56 ± 0.04 <sup>a</sup>
CV	29.7 ± 1.04 <sup>b</sup>	0.68 ± 0.03 <sup>b</sup>
CV-nanoemulsion	31.4 ± 2.34 <sup>b</sup>	0.7 ± 0.04 <sup>b</sup>
CV/Cisp	41.8 ± 2.07 <sup>a</sup>	1.9 ± 0.04 <sup>a</sup>
CV-nanoemulsion/Cisp	34.9 ± 2.07 <sup>a</sup>	1.5 ± 10.06

Values are represented as means ± SE for 6 rats in each group. <sup>a</sup> significant difference compared to the control group, <sup>b</sup> significant difference compared to cisp group. Significant at P < 0.05 (one-way ANOVA).

**Table 4.** Effect of CV and its nanoemulsion on hs-CRP, IL-6, and TNF-α in Cisp-induced nephrotoxicity in rats.

Groups	Hs-CRP (mg/l)	IL-6 (pg/ml)	TNF-α (pg/ml)
Control	36 ± 0.74	81.6 ± 0.8	67.6 ± 0.7
Cisp group	72.8 ± 1.07 <sup>a</sup>	133 ± 1.24 <sup>a</sup>	130 ± 2.24 <sup>a</sup>
CV	41.7 ± 0.8 <sup>b</sup>	79.6 ± 0.5 <sup>b</sup>	71.6 ± 0.5 <sup>b</sup>
CV-nanoemulsion	40.4 ± 0.9 <sup>b</sup>	84 ± 0.4 <sup>b</sup>	72 ± 0.6 <sup>b</sup>
CV/Cisp	62.8 ± 0.7 <sup>a</sup>	103 ± 0.5 <sup>a</sup>	75 ± 1.5 <sup>a</sup>
CV-nanoemulsion/Cisp	52.9 ± 0.78 <sup>a</sup>	92 ± 0.6	99 ± 2.4

Values are represented as means ± SE for 6 rats in each group. <sup>a</sup> significant difference compared to the control group, <sup>b</sup> significant difference compared to cisp-group. Significant at P < 0.05 (one-way ANOVA).

capsules are noticed (Figure 2). Examination of the positive control, kidney showed atrophy of the glomeruli, degeneration of the renal tubules, hemorrhage and inflammatory infiltration in the interstitial tissues (Figure 2-B). In rats that were given CV only, the histological investigation showed the tissue of glomeruli, and the renal tubules appeared more or less like normal form (Figure 2-C). Investigation kidney of rats giving CV-nanoemulsion only showed that the tissue of cortex appeared nearly the normal structure (Figure 2-D). On the other hand, kidneys of rats given CV and Cisp showed the tissue appear more or less like normal. The presence of inflammatory infiltration in the interstitial tissues was noticed (Figure 2-E). Moreover, the tissues appeared more or less like normal structure (Figure 2-F) in the rats treated with CV-nanoemulsion and Cisp.

### 3.6. Histopathological results of the liver tissue

The liver sections of the control rats showed a hepatic lobule architecture. The central vein in the lobule surrounded by the hepatocytes and with strongly eosinophilic granulated cytoplasm as well as distinct nuclei. The hepatic sinusoids are observed between the hepatocytes' strands (Figure 3-A). Histopathological examination of liver from +ve control showed congested portal tract. Inflammatory infiltration in the interstitial tissues edema and necrotic hepatocytes that surrounded the portal area was also seen (Figure 3-B). Microscopic investigation of liver from rats given CV only showed the tissue appeared more or less like normal (Figure 3-C). In the case of rats given CV-nanoemulsion only, the liver exhibited the nearly normal structure (Figure 3-D). In rats given CV and Cisp, liver tissue showed more or less like normal structure (Figure 3-E). On the other hand, rats given CV-nanoemulsion and Cisp showed the tissues of the liver appeared more or less like normal form (Figure 3-F).

### 3.7. Gene and protein expression results

The qRT-PCR was used for the characterization of the expressions of mouse LGALS3, VEGF, and CAV1 in kidney tissue. mRNA expressions were detected in kidney tissue for these genes. Expression levels of nephrotoxicity-related genes including LGALS3, VEGF, and CAV1 in

kidney tissue using qRT-PCR are summarized in (Figures 4 and 5). Expression levels of nephrotoxicity-related genes including LGALS3, VEGF, and CAV1 in kidney tissue using qRT-PCR were measured. The results revealed that the expression of LGALS3, VEGF, and CAV1 genes has a highly significant increment in only Cis treated group when compared to other treated groups (data not shown). In Cisp + CV treated group, the expression of these genes was significantly decreased when compared with Cisp treated animals (P < 0.001). In addition, there were differences among Cisp + nano treated group and the negative control and nano alone but not significant. The protein expression Western blot analysis exhibited that the LGALS3 and CAV1 are highly expressed only in Cisp + CV treated group when compared with other groups. There was no significant difference between Cisp + nano treated rats and negative control for both gene and protein expression.

### 3.8. CV-nano-encapsulation results

Sodium alginate is one of the most often utilized polymers as an encapsulating material because it can build a very adaptable matrix that is biocompatible and non-toxic for the preservation of essential oils. The extrusion method involved pouring a sodium alginate solution into calcium salt solution, resulting in emulsification method and external ionic gelation, which involves internal ionic gelation of alginate in water/oil emulsion [49]. Extrusion particles typically had diameters ranging from 500 μm to 3 mm. The formed particles size was determined by the needle diameter used for the solution dripping, the viscosity, and the alginate solution concentration, as well as the distance between the syringe and the calcium chloride solution [50]. When the union zone between the blocks of acid -L-guluronic (G) of one alginate molecule was physically attached to another acid -L-guluronic (G) block from another alginate molecule by calcium ions, gelation occurs. The egg-box model offers a glimpse of the construction (Figure 6) [51]. Between charged biopolymers with opposing charges, an electrostatic contact was developed. A CV molecule as a positive polyelectrolyte and a polysaccharide molecule as a negative polyelectrolyte were employed in most biopolymer systems [52]. When CV was combined with calcium alginate, a more stable capsule is formed, allowing for the creation of a double wall in the microcapsule as shown in Figure 6 [53].

## 4. Discussion

CV, a common safe compound for consumption, has been used in foods based upon the acceptance via the Federal Drug Administration [54]. Additionally, it might be a leading drug compound due to its therapeutic action against inflammation, malignant tumors, viral infections, and immunity diseases [14]. The present study aimed to investigate the potentialities of CV and its nanoemulsion to inhibit the development of Cisp-induced nephrotoxicity in rat models. Several studies reported that Cisp causes the development of several side effects including mainly the Reactive oxygen species (ROS) and oxidative stress [55]. The amount of superoxide anions and hydroxyl radicals caused the increasing of Cisp-induced oxidative stress. Excessive ROS could destroy cellular protein, lipids, and DNA under oxidative stress conditions, as well as regulation of survival signals [56]. The cytotoxic effects of Cisp into the tubular cells were occurred via multi complicated mechanisms, including oxidative stress, followed by inflammation and subsequent cell apoptosis and necrosis leading to renal dysfunction [12]. The ROS excessive production caused mechanistically by mitochondrial and DNA damage also inhibited the antioxidant enzymes such as SOD, CAT and GSH [57]. Cisp cytotoxic action was analogous to that of alkylating agents. When entering the cell, the chloride ion dissociates and leaves a reactive complex that reacts with water and then interacts with the DNA by forming covalent bonds, preferably at the N7 position of adenine and guanine [58]. Due to the shortest life span of ROS, it is very hard to be detected so ROS-related tissue destruction could be estimated by the final product of lipid peroxidation, such as MDA, which is reported as a

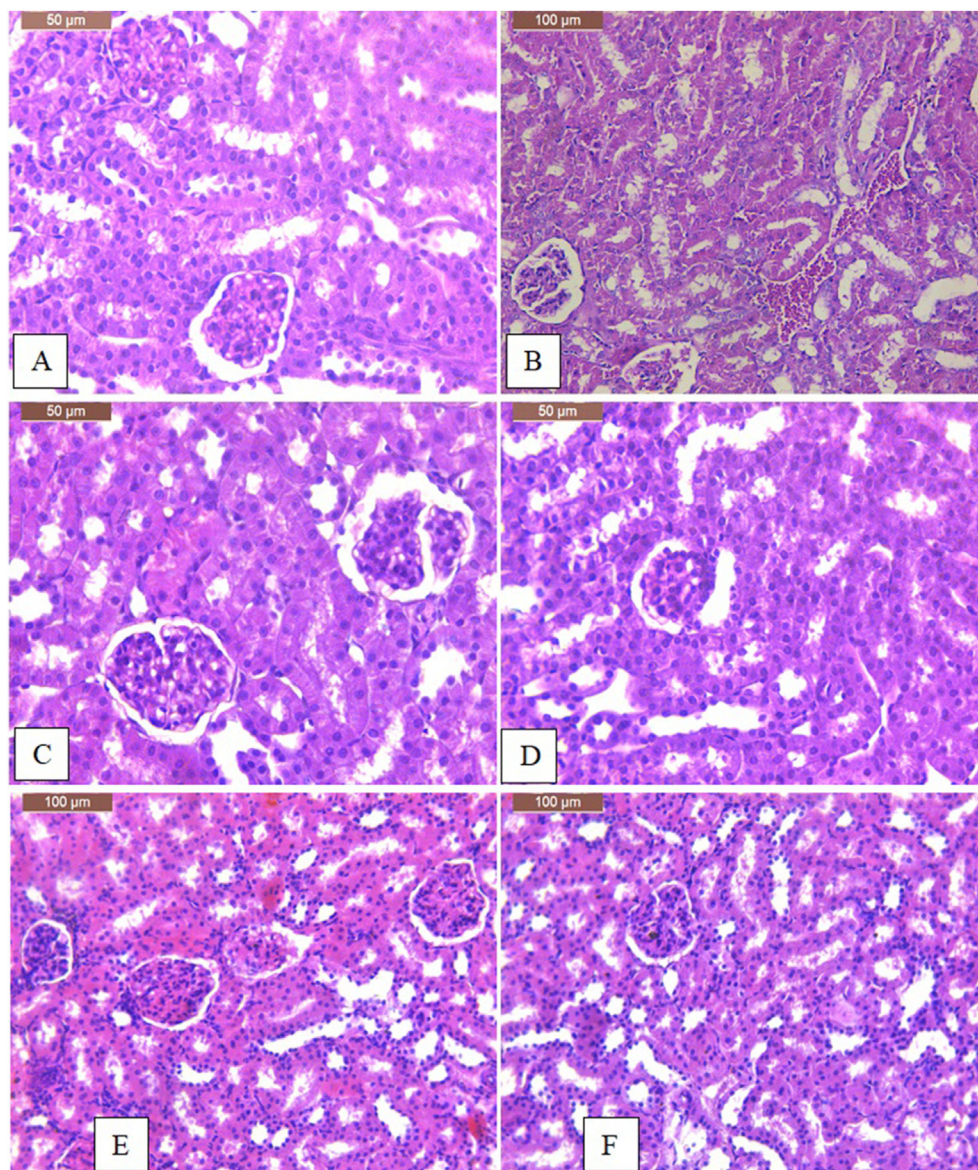


**Figure 2.** Sections of cortex tissues from rat's kidney of (A) control showed normal renal corpuscles, proximal convoluted tubules, and distal convoluted tubules. The glomeruli, urinary spaces, and Bowman's capsules are noticed (scale bar: 50  $\mu$ m), (B) Cisp group shows atrophy of the glomeruli, degeneration of the renal tubules, hemorrhage and inflammatory infiltration in the interstitial tissues, (C) rat given CV only shows the tissue appear more or less like normal, (D) rat given CV-nanoemulsion only shows the tissue appear nearly the normal structure, (E) rats given CV and Cisp shows the tissue appear more or less like normal. Notice the presence of inflammatory infiltration in the interstitial tissues, (F) rat given CV-nanoemulsion and Cisp shows the tissues appear more or less like normal (H & E stain, scale bar: 100  $\mu$ m).

realistic biomarker for measuring the level of oxidative stress [59, 60]. Our current hypotheses suggest that increased levels of MDA reported after Cisp administration were a consequence of its cytotoxicity and the development of oxidative stress. Measurement of the concentration of lipid peroxidation products and antioxidants may determine the level of tissue harm. Shalaby et al. [35], reported that MDA levels were controlled to normal by sodium salicylate dosage. The present analysis demonstrated that MDA return to decreased level after CV-nanoemulsion treatment when compared with Cisp group and this amelioration is more obvious than in the treatment with the CV alone.

There was also depletion of GSH as an important kidney free radical scavenger. Glutathione is the most abundant intracellular thiol and the ratio between its reduced (GSH) and oxidized (GSSG) forms largely determined the redox state of the cell [61]. The observed decreasing in kidney GSH following Cisp injection reflected the antioxidant consumption by the increasing of free radical generation and therefore substantially impair the kidney tissue ability to cope with further oxidative stress [62]. It was worth mentioning that glutathione is an essential source during that process for GSH-Px activity.

SOD is a crucial enzyme widely existing in the body. Its content can mirror free radicals scavenging ability [63]. The SOD could be postulated

as the start of sparks for antioxidant cascade by superoxide anion detoxification into hydrogen peroxide [64]. Then, the resulting compound will be converted to water by the succeeding enzymes, CAT and glutathione peroxidase (GSH-Px), to protect cells against ROS destructive action. With failing of these well-integrated endogenous antioxidant systems, the body could borrow these detoxification capacities by the assistant role of exogenous antioxidant molecules [64, 65, 66].

The current study referred that the CV or its nanoemulsion administration increased SOD and GSH. The SOD increases was found as corresponding with enhancement of resistance to oxidative stress. On the other hand, the Cisp group attained lower SOD activity when compared to the control group. It is possible that because of excessive production of free oxygen radicals, generating  $O_2^-$  and/or possible induction of SOD activity [67]. Furthermore, excessive  $O_2^-$  scavenges by SOD, so that the cells are protected against the toxic effects of superoxide radicals, reflecting the decrease in catalase enzyme activity. The effect of Cisp administration appeared in the decreasing in SOD activity That may be associated with the overproduction of oxidative stress, nitrosative stress, and the generation of oxygen [68].

Present observations indicated that the administration of either CV or its nanoemulsion ameliorated the Cisp-induced increasing in lipid

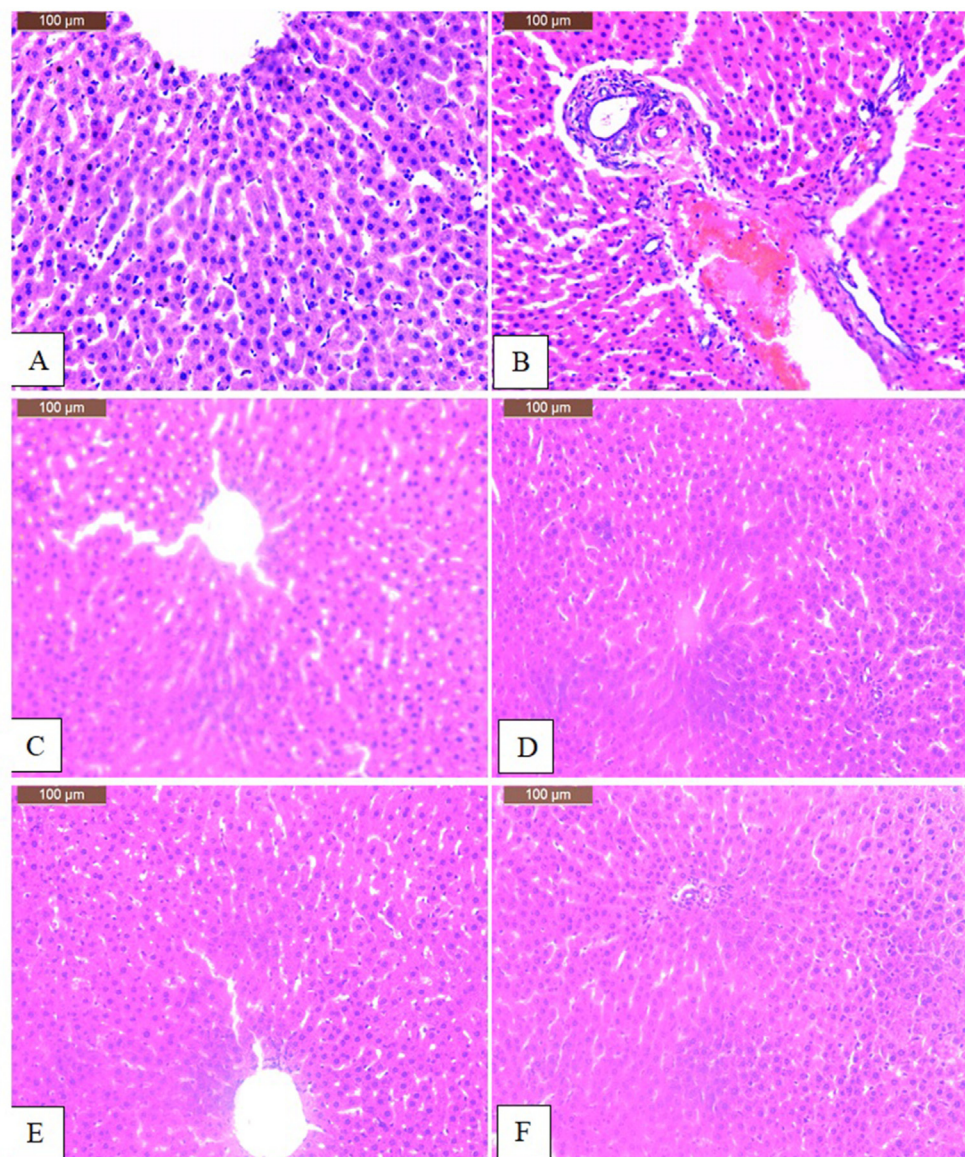


**Figure 3.** Sections of the liver of rats of (A) control show the normal architecture of a hepatic lobule. The central vein lies at the center of the lobule surrounded by the hepatocytes with strongly eosinophilic granulated cytoplasm, and distinct nuclei. Between the strands of hepatocytes, the hepatic sinusoids are shown, (B) Cisp group shows congested portal tract. Notice inflammatory infiltration in the interstitial tissues edema and necrotic hepatocytes that surrounded the portal area, (C) rat given CV only shows the tissue appear more or less like normal, (D) rat given CV-nanoemulsion only shows the tissue appear nearly the normal structure, (E) rat given CV and Cisp shows the tissue appear more or less like normal, (F) rat given CV-nanoemulsion and Cisp shows the tissues appear more or less like normal (H & E stain, scale bar: 100 μm).

peroxidation and counteracted the decrease in kidney GSH and SOD. Moreover, either drug-induced a significant decrease in the elevated MDA levels in the kidney of Cisp-treated rats. The effect of CV or its nanoemulsion on oxidative stress is likely to be of benefit in reducing nephron injury during the state of inflammation and oxidative stress. Here, it is worthy to mentioning that the CV-nanoemulsion model bears a structural antioxidant, which might underlie its antioxidant properties.

As mentioned above, the excessive increasing of the pro-inflammatory factors levels including the TNF- $\alpha$  and IL-6 are the main initiators of inflammatory cascade reaction of cis-induced nephrotoxicity. It could provoke glomerular vascular endothelial cells to secrete adhesion factors that endorse the proliferation of glomerular mesangial cells and thus glomerular lesions [63]. After stimulation by some antigens, the mesangial cells could sustainably secrete IL-6. Thus, the serum IL-6 level was significantly increased. The increased IL-6 could stimulate the proliferation of mesangial cells, induce the pathological changes of glomeruli and abnormal structure and function [67]. In addition, IL-6 could stimulate the kidney cells to produce a large number of hs-CRP, which aggravates the inflammatory response [69]. Herein, compared with the normal control group, the renal tissue TNF- $\alpha$ , IL-6, and hs-CRP levels in the Cisp-group were significantly increased. On the other

hand, the levels of these indexes were significantly reduced in CV and its nanoemulsion groups in which the decreasing is more obvious in the nanoemulsion group than CV group when compared with the control group. Basically, the inflammatory response was involved in nephrotoxicity rat models. Based upon these data, CV and especially its nanoemulsion form exhibited the potentialities of the reduction of the inflammatory response and thus reducing the renal injury.

The qRT-PCR was used for the characterization of mouse LGALS3, VEGF, and CAV1 expressions in kidney tissue. The mRNA expressions were detected in kidney tissue for these genes. Expression levels of nephrotoxicity-related genes including LGALS3, VEGF, and CAV1 in kidney tissue using qRT-PCR are summarized in (Table 4 and Figure 4, Fig. S1–S3). The results revealed that the expression of LGALS3, VEGF, and CAV1 genes were significantly increased ( $P < 0.001$ ) in Cisp only treated group when compared to the treated groups (negative control, CV-nano alone, and CV-nanoCV + Cisp treated tissues). In addition, there were differences between Cisp + CV-nano treated group and both of negative control and nano alone but was not significant. In parallel to gene expression data, the two proteins (LGALS3 and CAV1), analyzed by Western blot method, were found highly expressed only in Cisp treated group without significant differences between other groups.

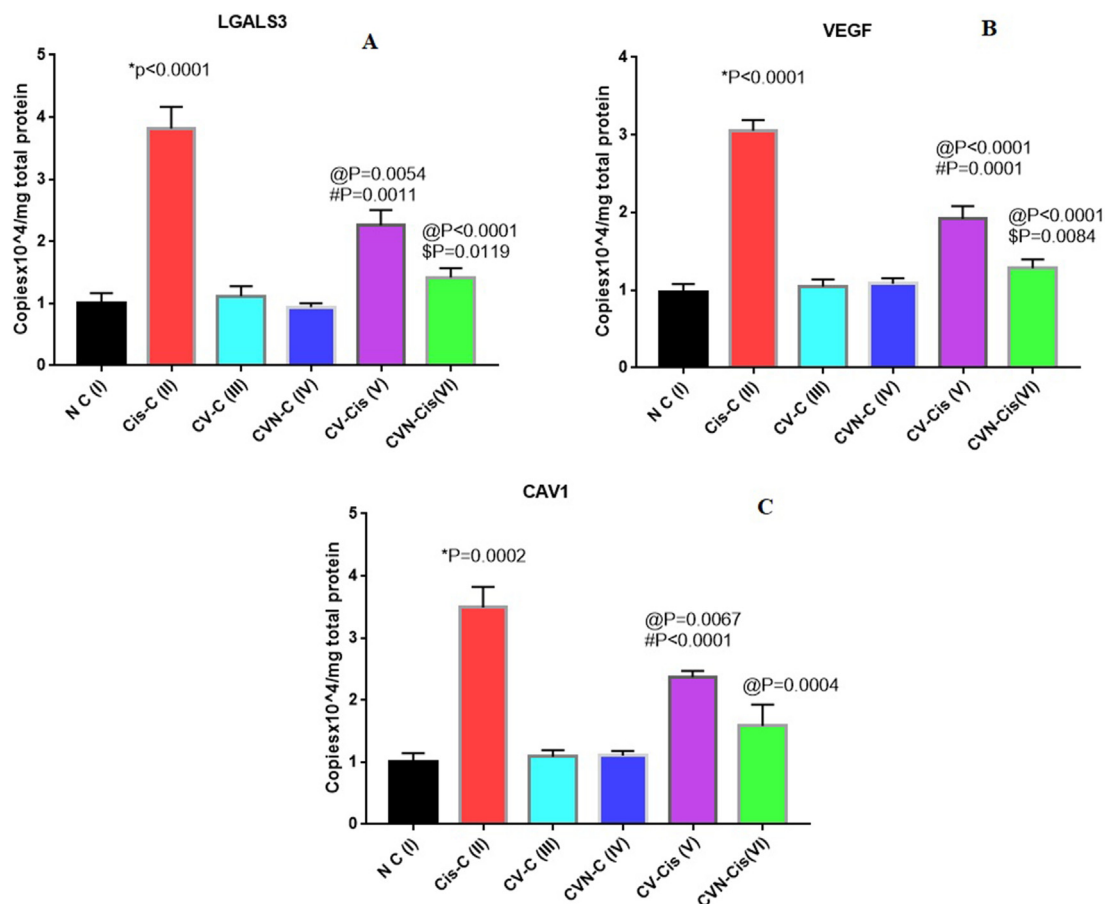


**Figure 4.** The RT-qPCR validation of mRNA expression for LGALS3, VEGF, and CAV1 in kidney tissue. \* indicated significant differences between means at  $P < 0.05$  and error bars represents standard error of the mean (SEM). Means comparisons were performed by using Duncan's multiple range test. Samples/group  $n = 06$ . Expression levels were normalized using  $\beta$ -actin levels.

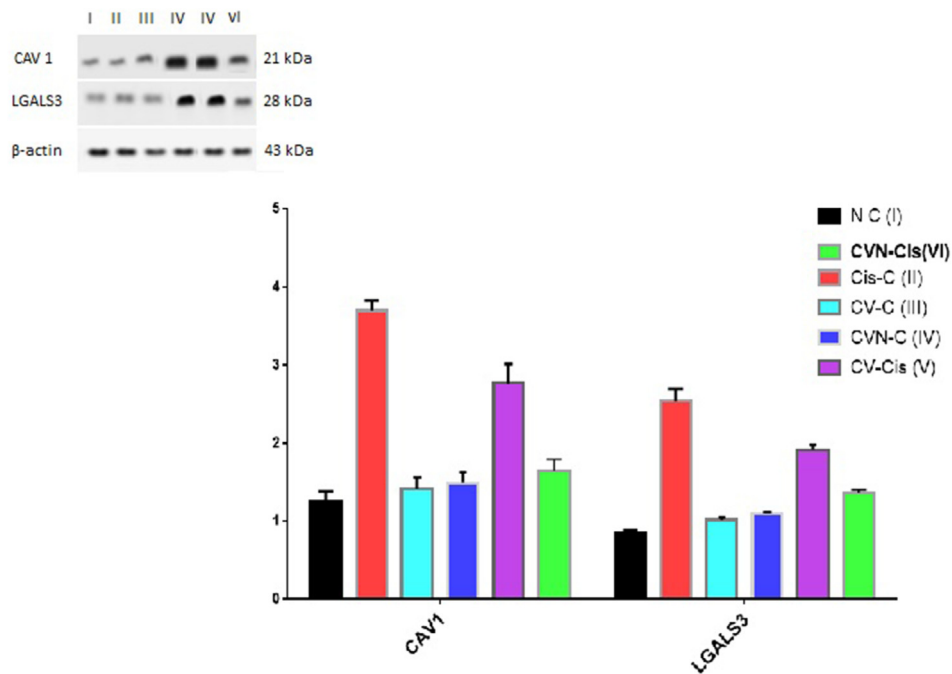


**Figure 5.** Protein expression of both CAV and LGALS3 in rat kidney tissues, Control (I), CV alone (II), CV-nanoemulsion alone (III), CV + Cisp (IV), and CV-nanoemulsion + Cisp (V). For Non-adjusted images (see fig. S1–S3).

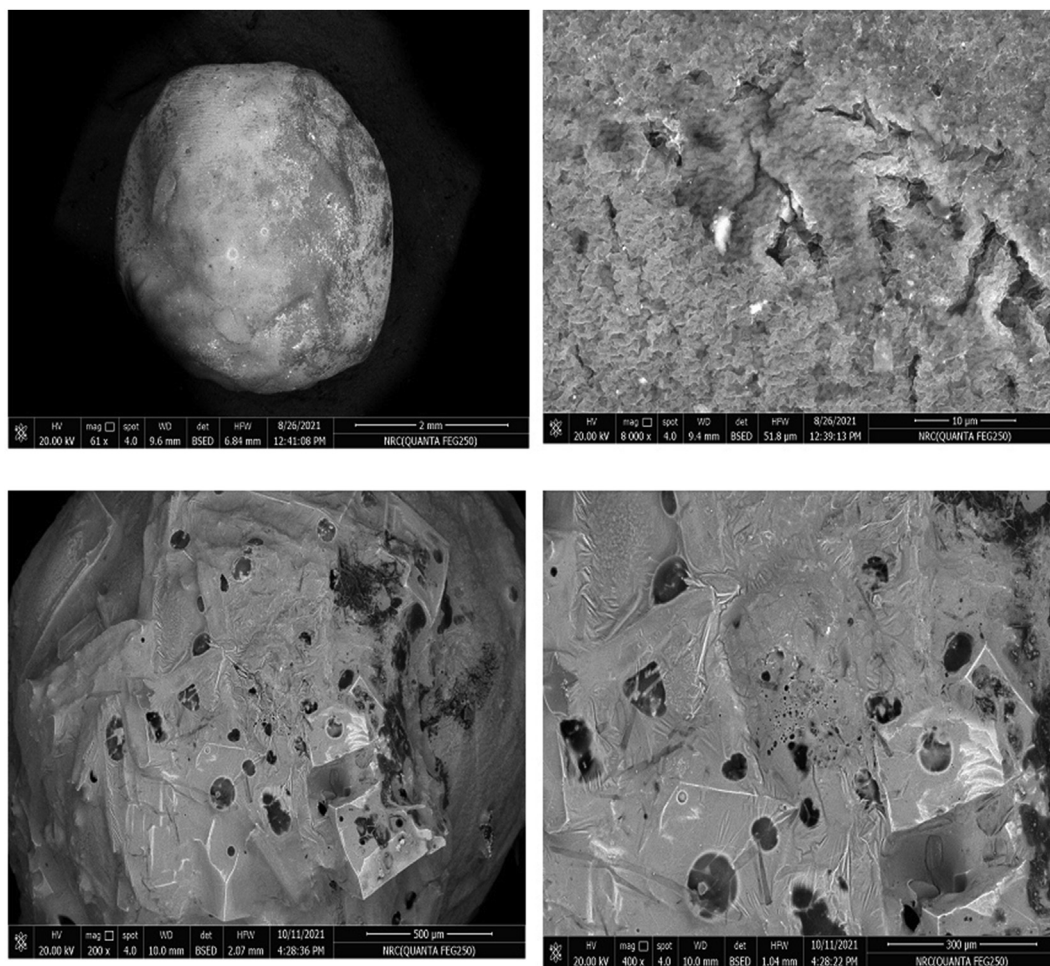


Figure 6. SEM of CV-nano-encapsulation particles.

Rui et al. [70] concluded that galectin-3 (LGALS3) serves significant roles in many biological activities, including cell growth, apoptosis, pre-mRNA splicing, differentiation, transformation, angiogenesis, inflammation, and fibrosis. Earlier studies have shown that galectin-3 may be used as a diagnostic or prognostic biomarker for certain types of heart disease, kidney disease, and cancer.

The LGALS3 might act for the regulation of the cell growth, differentiation, and inflammation through its carbohydrate-binding function. LGALS3 also played a complex context-dependent role in the kidneys. Szu-Chia and Po-Lin [71] suggested that a rise in the concentration of galectin-3 has been conveyed to be associated with renal fibrosis. Raised levels of plasma galectin-3 are also associated with increased risks of rapid renal function decline, incident chronic kidney disease, and progressive renal impairment.

Vascular endothelial growth factor (VEGF) is the main regulator of blood vessel growth and plays an important role in promoting endothelial survival and maintaining the microvasculature [72].

VEGF is elemental for endothelial cell differentiation (vasculogenesis) and the sprouting of new capillaries from preexisting vessels (angiogenesis). In addition, there is a strong suggestion that VEGF is a survival factor allowing the cells to survive and proliferate under conditions of extreme stress [73]. Caveolin-1 (Cav1) acts a main role in the caveolae formation. Little is known about their functional role in the kidney. Caveolae have been involved in the regulation of vascular tone, cardiac rhythm, respiratory function, and overall lipid metabolism [73]. Cav1 and Cavin-1 (also known as Polymerase I and Transcript Release Factor; PTRF) are essential for the biogenesis of caveolae. Genetic deletion of either Cav1 or PTRF in

mice leads to impaired caveolae formation with resulting functional disorders primarily affecting blood vessels, lungs, and fat tissue [74]. In agreement with documented studies [73, 74], CV-nanoemulsion exhibited effective reduction of the expression of LGALS3, VEGF, and Cav1 which were increased in case of administration of Cisplatin.

Based upon these findings that deduced the significant effects of CV and its nanoemulsion, the nano-encapsulated form of the CV was prepared that might be reported as a starting drug leader. Sodium alginate was utilized as an encapsulating material because it builds a very adaptable matrix that is biocompatible and non-toxic for the preservation of CV-encapsulation of CV can open up Reverso's context of new drug delivery applications.

## 5. Conclusion

In addition to the previous documented significant biological potentialities of CV, our finding deduced the important effects of CV and its nanoemulsion as cytoprotectors against Cisplatin-induced nephrotoxicity in rats. These conclusions were constructed via their significant potentialities of them, especially CV-nanoemulsion, via improvement of the kidney SOD and GSH, in CV and the increasing of the serum urea, creatinine compared to NC animals indicating a better improvement comparing with the control and +ve groups. All these data were supported by histopathological analysis, gene expressions and Western blot. Finally and base these results, the microcapsulated form of CV was constructed that might be used as a unit for drug manufacture.

## Declarations

### Author contribution statement

All authors listed have significantly contributed to the development and the writing of this article.

### Funding statement

This research did not receive any specific grant from funding agencies in the public, commercial, or not-for-profit sectors.

### Data availability statement

Data included in article/supplementary material/referenced in article.

### Declaration of interests statement

The authors declare no conflict of interest.

### Additional information

Supplementary content related to this article has been published online at <https://doi.org/10.1016/j.heliyon.2022.e09198>.

### Acknowledgements

The authors gratefully acknowledge the National Research Centre, Egypt for the research support.

### References

- M.H. Rosner, M.A. Perazella, Acute kidney injury in patients with cancer, *N. Engl. J. Med.* 376 (2017) 1770–1781.
- M.L.C. Santos, B.B. de Brito, F.A.F. da Silva, A.C. dos S Botelho, F.F. de Melo, Nephrotoxicity in cancer treatment: an overview, *World J. Clin. Oncol.* 11 (2020) 190–204.
- H. Wu, J. Huang, Drug-induced nephrotoxicity: pathogenic mechanisms, biomarkers and prevention strategies, *Curr. Drug Metabol.* 19 (2018) 559–567.
- C.J. Lote, L. Harper, C.O. Savage, Mechanisms of acute renal failure, *Br. J. Anaesth.* 77 (1996) 82–89.
- V. Fanos, L. Cataldi, Renal transport of antibiotics and nephrotoxicity: a review, *J. Chemother.* 13 (2001) 461–472.
- P. Fisel, O. Renner, A.T. Nies, M. Schwab, E. Schaeffeler, Solute carrier transporter and drug-related nephrotoxicity: the impact of proximal tubule cell models for preclinical research, *Expet Opin. Drug Metabol. Toxicol.* 10 (2014) 395–408.
- C.A. Naughton, Drug-induced nephrotoxicity, *Am. Fam. Physician* 78 (2008) 743–750.
- S.G. Coca, S. Singanamala, C.R. Parikh, Chronic kidney disease after acute kidney injury: a systematic review and meta-analysis, *Kidney Int.* 81 (2012) 442–448.
- H.S. Kohli, M.C. Bhaskaran, T. Muthukumar, K. Thennarasu, K. Sud, V. Jha, K.L. Gupta, V. Sakhuja, Treatment-related acute renal failure in the elderly: a hospital-based prospective study, *Nephrol. Dial. Transplant.* 15 (2000) 212–217.
- Q. Ma, S.R. Devarajan, P. Devarajan, Amelioration of cisplatin-induced acute kidney injury by recombinant neutrophil gelatinase-associated lipocalin, *Ren. Fail.* 38 (2016) 1476–1482.
- Y. Kawai, S. Taniuchi, S. Okahara, M. Nakamura, M. Gemba, Relationship between cisplatin or nedaplatin-induced nephrotoxicity and renal accumulation, *Biol. Pharm. Bull.* 28 (2005) 1385–1388.
- I. Arany, R.L. Safirstein, Cisplatin nephrotoxicity, in: *Semin. Nephrol.*, Elsevier, 2003, pp. 460–464.
- S. Sharma, S. Baboota, S. Amin, S.R. Mir, Ameliorative effect of a standardized polyherbal combination in methotrexate-induced nephrotoxicity in the rat, *Pharm. Biol.* 58 (2020) 184–199.
- M. Sharifi-Rad, E.M. Varoni, M. Iriti, M. Martorell, W.N. Setzer, M. del Mar Contreras, B. Salehi, A. Soltani-Nejad, S. Rajabi, M. Tajbakhsh, Carvacrol and human health: a comprehensive review, *Phyther. Res.* 32 (2018) 1675–1687.
- S.E. Kintzios, Oregano: the Genera *Origanum* and *Lippia*, CRC Press, 2002.
- F.C. Fachini-Queiroz, R. Kummer, C.F. Estevao-Silva, M.D. de B. Carvalho, J.M. Cunha, R. Grespan, C.A. Bersani-Amado, R.K.N. Cuman, Effects of thymol and carvacrol, constituents of *Thymus vulgaris* L. essential oil, on the inflammatory response, Evidence-Based Complement, *Alternative Med.* 2012 (2012).
- X. Tang, S. Chen, L. Wang, Purification and identification of carvacrol from the root of *Stellera chamaejasme* and research on its insecticidal activity, *Nat. Prod. Res.* 25 (2011) 320–325.
- P.S. Chavan, S.G. Tupe, Antifungal activity and mechanism of action of carvacrol and thymol against vineyard and wine spoilage yeasts, *Food Control* 46 (2014) 115–120.
- W. Du, C.W. Olsen, R.J. Avena-Bustillos, T.H. McHugh, C.E. Levin, M. Friedman, Antibacterial activity against *E. coli* O157: H7, physical properties, and storage stability of novel carvacrol-containing edible tomato films, *J. Food Sci.* 73 (2008) M378–M383.
- A. Nostro, A.R. Blanco, M.A. Cannatelli, V. Enea, G. Flamini, I. Morelli, A. Sudano Roccaro, V. Alonzo, Susceptibility of methicillin-resistant staphylococci to oregano essential oil, carvacrol and thymol, *FEMS Microbiol. Lett.* 230 (2004) 191–195.
- D.H. Gilling, M. Kitajima, J.R. Torrey, K.R. Bright, Antiviral efficacy and mechanisms of action of oregano essential oil and its primary component carvacrol against murine norovirus, *J. Appl. Microbiol.* 116 (2014) 1149–1163.
- C. Sánchez, R. Aznar, G. Sánchez, The effect of carvacrol on enteric viruses, *Int. J. Food Microbiol.* 192 (2015) 72–76.
- K.M. Arunasree, Anti-proliferative effects of carvacrol on a human metastatic breast cancer cell line, MDA-MB 231, *Phytomedicine* 17 (2010) 581–588.
- A. Özkan, A. Erdoğan, A comparative evaluation of antioxidant and anticancer activity of essential oil from *Origanum onites* (Lamiaceae) and its two major phenolic components, *Turkish J. Biol.* 35 (2011) 735–742.
- Q. Yin, F. Yan, X.-Y. Zu, Y. Wu, X. Wu, M. Liao, S. Deng, L. Yin, Y. Zhuang, Anti-proliferative and pro-apoptotic effect of carvacrol on human hepatocellular carcinoma cell line HepG-2, *Cytotechnology* 64 (2012) 43–51.
- B. Aristatile, K.S. Al-Numair, A.H. Al-Assaf, K.V. Pugalendi, Pharmacological effect of carvacrol on D-galactosamine-induced mitochondrial enzymes and DNA damage by single-cell gel electrophoresis, *J. Nat. Med.* 65 (2011) 568–577.
- A.G. Guimarães, G.F. Oliveira, M.S. Melo, S.C.H. Cavalcanti, A.R. Antonioli, L.R. Bonjardim, F.A. Silva, J.P.A. Santos, R.F. Rocha, J.C.F. Moreira, Bioassay-guided evaluation of antioxidant and antinociceptive activities of carvacrol, *Basic Clin. Pharmacol. Toxicol.* 107 (2010) 949–957.
- M. Milos, D. Makota, Investigation of antioxidant synergisms and antagonisms among thymol, carvacrol, thymoquinone and p-cymene in a model system using the Briggs–Rauscher oscillating reaction, *Food Chem.* 131 (2012) 296–299.
- B. Aristatile, K.S. Al-Numair, C. Veeramani, K.V. Pugalendi, Effect of carvacrol on hepatic marker enzymes and antioxidant status in d-galactosamine-induced hepatotoxicity in rats, *Fundam. Clin. Pharmacol.* 23 (2009) 757–765.
- D.J. Son, Y.H. Park, Y.M. Kim, N.H. Chung, H.S. Lee, Antiplatelet activity of *Thujopsis dolabrata* var. *hondai*-derived component against platelet aggregation, *J. Microbiol. Biotechnol.* 15 (2005) 425–427.
- S. Aydin, A.A. Başaran, N. Başaran, Modulating effects of thyme and its major ingredients on oxidative DNA damage in human lymphocytes, *J. Agric. Food Chem.* 53 (2005) 1299–1305.
- A.H. Klein, M.I. Carstens, E. Carstens, Eugenol and carvacrol induce temporally desensitizing patterns of oral irritation and enhance innocuous warmth and noxious heat sensation on the tongue, *PAIN®*. 154 (2013) 2078–2087.
- A.I. Elshamy, N.M. Ammar, H.A. Hassan, S.L. Al-Rowaily, T.I. Ragab, A.E.-N.G. El Gendy, A.M. Abd-ElGawad, Essential oil and its nanoemulsion of *Araucaria heterophylla* resin: chemical characterization, anti-inflammatory, and antipyretic activities, *Ind. Crop. Prod.* 148 (2020) 112272.
- H.M.I. Abdallah, N.M. Ammar, M.F. Abdelhameed, A.E.-N.G. El Gendy, T.I.M. Ragab, A.M. Abd-ElGawad, M.A. Farag, M.S. Alwahibi, A.I. Elshamy, Protective mechanism of *Acacia saligna* butanol extract and its nano-formulations against ulcerative colitis in rats as revealed via biochemical and metabolomic assays, *Biology* 9 (2020).
- M.A. Shalaby, A.A.H. Abdel-Rahman, I.F. Zeid, E.R. Youness, N.A. Mohamed, Protective effect of drug loaded nanoparticles on brain toxicity in experimental animals, *Egypt, J. Chem.* 64 (2021) 3265–3273.
- S.A.E. Bashandy, A. Salama, A.M. Fayed, E.A. Omara, S.A. El-Toumy, J.Y. Salib, Protective effect of Mandrin (*Citrus Reticulata*) peel extract on potassium dichromate induced hepatotoxicity and nephrotoxicity in rats, *Plant Arch* 20 (2020) 2231–2242.
- M.F. El-Refaei, E.A.A. Abdallah, Protective effects of caffeic acid phenethyl ester on cadmium-induced testicular injury: a crucial role of antioxidant enzymes in male mice infertility, *Heliyon* 7 (2021), e06965.
- S.S. Mohamed, A.H.M. Fayed, Anti-obesity synergistic effect of pomegranate seed oil (PSO) and Arabic gum (AG) in Albino Rats, *Int. J. Vet. Sci.* 9 (2020) 84–89.
- A. Salama, M.F. Abdelhameed, S. Mostafa, S.A. Nada, H.S. Taha, A.A. Amer, Influence of extract derived cell cultures of broccoli against osteoporosis in ovariectomized rats, *Egypt, J. Chem.* 64 (2021) 3521–3539.
- S.S. Abd El-Karim, H.S. Mohamed, M.F. Abdelhameed, A. El-Galil E. Amr, A.A. Almezizia, E.S. Nossier, Design, synthesis and molecular docking of new pyrazole-thiazolidinones as potent anti-inflammatory and analgesic agents with TNF- $\alpha$  inhibitory activity, *Bioorg. Chem.* 111 (2021).
- A.M. Ghanim, A.S. Girgis, B.M. Kariuki, N. Samir, M.F. Said, Bioorganic Chemistry Design and Synthesis of Ibuprofen-Quinoline Conjugates as Potential Anti-inflammatory and Analgesic Drug Candidates 119, 2022.
- S.A. Sakyi, A. Enimil, D.K. Adu, R.D. Ephraim, K.O. Danquah, L. Fondjo, D. Baidoo-Ansah, P. Adoba, E. Toboh, B.O. Afranie, Individual and combined bioscore model of presepsin, procalcitonin, and high sensitive C-reactive protein as biomarkers for early diagnosis of paediatric sepsis, *Heliyon* 6 (2020), e04841.
- M.F. Abdelhameed, G.F. Asaad, T.I.M. Ragab, R.F. Ahmed, A.E.-N.G. El Gendy, S.S. Abd El-Rahman, A.M. Elgamal, A.I. Elshamy, Oral and topical anti-inflammatory and antipyretic potentialities of *Araucaria bidivillii* shoot essential oil and its nanoemulsion in relation to chemical composition, *Molecules* 26 (2021) 5833.

- [44] M. Shalaby, A. Abdel-Rahman, I. Zaid, E. Youness, N. Mohamed, Protective effect of drug loaded nanoparticles on brain toxicity in experimental animals, Egypt, *J. Chem.* (2021).
- [45] A.-T.H. Mossa, S.I. Afia, S.M.M. Mohafresh, B.A. Abou-Awad, Formulation and characterization of garlic (*Allium sativum* L.) essential oil nanoemulsion and its acaricidal activity on eriophyid olive mites (Acari: eriophyidae), *Environ. Sci. Pollut. Res.* 25 (2018) 10526–10537.
- [46] S. Sugumar, S.K. Clarke, M.J. Nirmala, B.K. Tyagi, A. Mukherjee, N. Chandrasekaran, Nanoemulsion of eucalyptus oil and its larvicidal activity against *Culex quinquefasciatus*, *Bull. Entomol. Res.* 104 (2014) 393–402.
- [47] I. Motta Felício, R. Limongi de Souza, C. Oliveira Melo, K.Y. Gervázio Lima, U. Vasconcelos, R. Olímpio de Moura, E. Eleamen Oliveira, Development and characterization of a carvacrol nanoemulsion and evaluation of its antimicrobial activity against selected food-related pathogens, *Lett. Appl. Microbiol.* 72 (2021) 299–306.
- [48] C. Fernandes, F. de Almeida, A. Silveira, M. Gonzalez, C. Mello, D. Feder, R. Apolinário, M. Santos, J.C. Carvalho, L.A. Tietbohl, L. Rocha, D. Falcão, Development of an insecticidal nanoemulsion with *Manilkara subsericea* (Sapotaceae) extract, *J. Nanobiotechnol.* 12 (2014) 22.
- [49] W. Gombotz, Protein release from alginate matrices, *Adv. Drug Deliv. Rev.* 31 (1998) 267–285.
- [50] P. Burey, B.R. Bhandari, T. Howes, M.J. Gidley, Hydrocolloid gel particles: formation, characterization, and application, *Crit. Rev. Food Sci. Nutr.* 48 (2008) 361–377.
- [51] K.I. Draget, B. Strand, M. Hartmann, S. Valla, O. Smidsrød, G. Skjåk-Bræk, Ionic and acid gel formation of epimerised alginates; the effect of AlgE4, *Int. J. Biol. Macromol.* 27 (2000) 117–122.
- [52] X. Jun-xia, Y. Hai-yan, Y. Jian, Microencapsulation of sweet orange oil by complex coacervation with soybean protein isolate/gum Arabic, *Food Chem.* 125 (2011) 1267–1272.
- [53] M. Chávarri, I. Marañón, R. Ares, F.C. Ibáñez, F. Marzo, M. del C. Villarán, Microencapsulation of a probiotic and prebiotic in alginate-chitosan capsules improves survival in simulated gastro-intestinal conditions, *Int. J. Food Microbiol.* 142 (2010) 185–189.
- [54] H. Javed, M.F.N. Meeran, N.K. Jha, S. Ojha, Carvacrol, a plant metabolite targeting viral protease (mpro) and ACE2 in host cells can be a possible candidate for COVID-19, *Front. Plant Sci.* 11 (2021) 2237. <https://www.frontiersin.org/article/10.3389/fpls.2020.601335>.
- [55] V.N. Ayyagari, T.J. Hsieh, P.L. Diaz-Sylvester, L. Brard, Evaluation of the cytotoxicity of the Bithionol - cisplatin combination in a panel of human ovarian cancer cell lines, *BMC Cancer* 17 (2017) 49.
- [56] Q. Qian, W. Chen, Y. Cao, Q. Cao, Y. Cui, Y. Li, J. Wu, Targeting Reactive Oxygen Species in Cancer via Chinese Herbal Medicine, 2019.
- [57] X. Yu, X. Meng, M. Xu, X. Zhang, Y. Zhang, G. Ding, S. Huang, A. Zhang, Z. Jia, Celastrol ameliorates cisplatin nephrotoxicity by inhibiting NF- $\kappa$ B and improving mitochondrial function, *EBioMedicine* 36 (2018) 266–280.
- [58] M.B. Visacri, E. de C. Pincinato, G.B. Ferrari, J.C.F. Quintanilha, P.G. Mazzola, C.S.P. Lima, P. Moriel, Adverse drug reactions and kinetics of cisplatin excretion in urine of patients undergoing cisplatin chemotherapy and radiotherapy for head and neck cancer: a prospective study, *DARU J. Pharm. Sci.* 25 (2017) 12.
- [59] C.C. Tsai, H.S. Chen, S.L. Chen, Y.P. Ho, K.Y. Ho, Y.M. Wu, C.C. Hung, Lipid peroxidation: a possible role in the induction and progression of chronic periodontitis, *J. Periodontol. Res.* 40 (2005) 378–384.
- [60] D.A. Cherian, T. Peter, A. Narayanan, S.S. Madhavan, S. Achamma, G.P. Vynat, Malondialdehyde as a marker of oxidative stress in periodontitis patients, *J. Pharm. BioAllied Sci.* 11 (2019) S297–S300.
- [61] S.S. El-Hawary, W.E. Hammam, M. El-Mahdy El-Tantawi, N.A.Z. Yassin, F.N. Kirolos, M.F. Abdelhameed, M.A.O. Abdelfattah, M. Wink, M. Sobeh, Apple leaves and their major secondary metabolite phlorizin exhibit distinct neuroprotective activities: evidence from in vivo and in silico studies, *Arab. J. Chem.* 14 (2021).
- [62] B. Halliwell, Biochemistry of oxidative stress, *Biochem. Soc. Trans.* 35 (2007) 1147–1150.
- [63] X. Wang, Z. Li, X. Huang, F. Li, J. Liu, Z. Li, D. Bai, An experimental study of exenatide effects on renal injury in diabetic rats, *Acta Cir. Bras.* 34 (2019).
- [64] M.L. Urso, P.M. Clarkson, Oxidative stress, exercise, and antioxidant supplementation, *Toxicology* 189 (2003) 41–54.
- [65] H. Pekmez, M. Ogeturk, H. Ozyurt, M.F. Sonmez, N. Colakoglu, I. Kus, Ameliorative effect of caffeic acid phenethyl ester on histopathological and biochemical changes induced by cigarette smoke in rat kidney, *Toxicol. Ind. Health* 26 (2010) 175–182.
- [66] G. Serarslan, E. Altuğ, T. Kontas, E. Atik, G. Avci, Caffeic acid phenethyl ester accelerates cutaneous wound healing in a rat model and decreases oxidative stress, *Clin. Exp. Dermatol.* 32 (2007) 709–715.
- [67] M. Ji, Y. Lu, C. Zhao, W. Gao, F. He, J. Zhang, D. Zhao, W. Qiu, Y. Wang, C5a induces the synthesis of IL-6 and TNF- $\alpha$  in rat glomerular mesangial cells through MAPK signaling pathways, *PLoS One* 11 (2016), e0161867.
- [68] A. Altuntaş, H.R. Yılmaz, A. Altuntaş, E. Uz, M. Demir, A. Gökçimen, O. Aksu, D.Ş. Bayram, M.T. Sezer, Caffeic acid phenethyl ester protects against amphotericin B induced nephrotoxicity in rat model, *BioMed Res. Int.* 2014 (2014) 1–8.
- [69] X.H. Wang, S.Q. Liu, Y.L. Wang, Y. Jin, Correlation of serum high-sensitivity C-reactive protein and interleukin-6 in patients with acute coronary syndrome, *Genet. Mol. Res.* 13 (2014) 4260–4266.
- [70] R. Dong, M. Zhang, Q. Hu, S. Zheng, A. Soh, Y. Zheng, H. Yuan, Galectin-3 as a novel biomarker for disease diagnosis and a target for therapy, *Int. J. Mol. Med.* 41 (2018) 599–614.
- [71] S.-C. Chen, P.-L. Kuo, The role of galectin-3 in the kidneys, *Int. J. Mol. Sci.* 17 (2016) 565.
- [72] K.E. Pinkerton, M.J. Herring, D.M. Hyde, F.H.Y. Green, Normal aging of the lung, in: *Lung*, Elsevier, 2014, pp. 265–285.
- [73] B.-S. Kim, M.S. Goligorsky, Role of VEGF in kidney development, microvascular maintenance and pathophysiology of renal disease, *Korean J. Intern. Med. (Engl. Ed.)* 18 (2003) 65.
- [74] L. Liu, D. Brown, M. McKee, N.K. LeBrasseur, D. Yang, K.H. Albrecht, K. Ravid, P.F. Pilch, Deletion of Cav1/PTRF causes global loss of caveolae, dyslipidemia, and glucose intolerance, *Cell Metabol.* 8 (2008) 310–317.